Global Journal of Science Frontier Research: B Chemistry
Volume 19 Issue 2 Version 1.0 Year 2019
Type : Double Blind Peer Reviewed International Research Journal
Publisher: Global Journals
Online ISSN: 2249-4626 & Print ISSN: 0975-5896

Natural Products for Material Protection: Passivation Enhancing Potentials of *Spondias Mombin* as AISI 316L Corrosion Inhibitor in 3.5% NaCl Solution

By Raphael S. Oguike & Omolara Oni
Abubakar Tafawa Balewa University

Abstract- The corrosion inhibition characteristics of *Spondias mombin* (SM) on stainless steel AISI 316L in 3.5% NaCl has been studied using gasometric, potentiodynamic polarization, surface and elemental analysis and computational techniques. Results showed that the inhibition occurs through adsorption of the inhibitor molecules on the metal surface. The effectiveness of protection became more pronounced with decreasing gas evolution as extract concentration increased. Electrochemical results revealed that the extracts' constituents adsorbed on the AISI 316L surface and enhanced the passivation mechanism which is in agreement with the reduced the anodic and cathodic current densities. Computational simulations were adopted to describe probable reactiveness of SM leaf extract constituents on Fe(110) slab.

Keywords: corrosion inhibition, stainless steel, spondias mombin, elemental analysis, passivation enhancer, adsorption.

GJSFR-B Classification: FOR Code: 030599

Natural Products for Material Protection: Passivation Enhancing Potentials of *Spondias Mombin* as AISI 316L Corrosion Inhibitor in 3.5% NaCl Solution

Raphael S. Oguike [α] & Omolara Oni [σ]

Abstract- The corrosion inhibition characteristics of *Spondias mombin* (SM) on stainless steel AISI 316L in 3.5% NaCl has been studied using gasometric, potentiodynamic polarization, surface and elemental analysis and computational techniques. Results showed that the inhibition occurs through adsorption of the inhibitor molecules on the metal surface. The effectiveness of protection became more pronounced with decreasing gas evolution as extract concentration increased. Electrochemical results revealed that the extracts' constituents adsorbed on the AISI 316L surface and enhanced the passivation mechanism which is in agreement with the reduced the anodic and cathodic current densities. Computational simulations were adopted to describe probable reactiveness of SM leaf extract constituents on Fe(110) slab.

Keywords: corrosion inhibition, stainless steel, spondias mombin, elemental analysis, passivation enhancer, adsorption.

I. Introduction

Protection of stainless steel that finds service in several sectors of the economy has been of keen interest, especially the media which includes chloride ions [1]. AISI 316L type stainless steel are used in marine-relative environment and various engineering applications owing their excellent corrosion resistant properties, high ductility, aesthetic appearance and high work hardening rate [2-6]. However, when in contact with medium containing chloride ions, they are much susceptible to corrosion, leading to enormous economic losses and pose potential safety problems. These challenges are contained by the use of corrosion inhibitors to lengthen their in-service years. Most commercial corrosion inhibitors function as passivation enhancers via forming monoatomic or polyatomic oxide film on the metal surface which results in a reduction of corrosion reaction and metal surface protection. However, the main drawback is the toxicity, cost and carcinogenic nature of inhibitors involving chromates [7]. This has led to the investigation of alternative compounds that are environmentally acceptable and offer effective corrosion protection as well as enhance the metal's passivation potential.

Of the efficient methods to protect against corrosive attacks on AISI 316L deployed in service is the use of organic compounds which contain conjugated double bonds, triple bonds and electronegative species to form tight surface films [8–13].Numerous advancements have been made to address the growing need for proficient inhibition for stainless steel corrosion in a bid to find inhibitors of natural product origin [14]. Natural products of plant origin contain organic constituents with similar structures as the commercial inhibitors having aromatic rings, multiple bonds, electronegative functional groups as well as hetero-atoms like nitrogen, sulfur and oxygen in their molecular backbone. These species are beneficial to form complex chelating ligands with the metal surface against corrosive species, as they are regarded as major adsorption centers within the inhibitor molecule that form compact thin film on the metal.

The basis for corrosion control is a compromise between the benefits generated by the level of corrosion control versus the costs that would result if that level of control were not maintained Regrettably, several of these commercial inhibitors are expensive, toxic and hazardous to environment [15-16], hence the drive to develop eco-friendly corrosion inhibitors with adequate effectiveness and efficiency [17]. An attempt has been made in the present work to describe the inhibitory features and efficiency of *Spondias mombin* for corrosion of AISI 316L in 3.5% NaCl solutions.

II. Experimental

a) Material Preparation

The composition of AISI 316L which was obtained commercially from Advent research materials Ltd, England OX294JA has the following typical analysis (ppm) C < 300, Si <100, Ni < 1400, Mn < 200, Cr < 1800, Mo < 300, S < 300, P < 450 and Fe. The sheets were reduced to specimens mechanically and treated as described in our earlier work as well as inhibitor preparation [5].

Author α σ: Corrosion Protection and Materials Laboratory, Department of Chemistry, Abubakar Tafawa Balewa University, Bauchi, Nigeria. e-mails: oguike.raphael@yahoo.com, oraphael@atbu.edu.ng

b) Gasometric Measurement

In the gasometric method, seventy milliliters of 2 M HCl solution without and with AM leaf extracts was introduced into the gasometric apparatus. AISI 316L specimen was introduced into the flask which was quickly corked. The initial volume of paraffin oil in the apparatus was recorded. The decrease in volume of the paraffin oil due to hydrogen gas evolution was taken after every five minutes. From the volume of hydrogen gas evolved, the corrosion rate was calculated using eqn (2) while the inhibition efficiency of the inhibitor was calculated using eqn (3) [5].

$$CR_{HE} = \frac{V_f - V_i}{t_f - t_i} \quad (1)$$

$$IE_{HE}\% = 1 - \frac{CR_{HE\ (in\ hib)}}{CR_{HE\ (free\ )}} \quad (2)$$

where CRHE is the corrosion rate, Vf and Vi is the final and initial volume of gas evolved, tf and ti the final and initial time in minutes and CRHE(inhib) and CRHE(free) are corrosion rates in the presence and absence of the inhibitor.

c) Electrochemical Measurement

A polarization cell with a three-electrode configuration was used for electrochemical measurements; steel specimens having a total exposed surface area of 1cm2 was used as working electrode, a graphite rod and a saturated calomel electrode (SCE) were used as counter and reference electrode respectively. The working electrode was used as obtained, however, were cleaned with distilled water, degreased with ethanol, and finally dried with acetone and warm air. Electrochemical experiments were conducted using a VERSASTAT 3 Complete DC Voltammeter and Corrosion System as described in [15]. The inhibition efficiency was calculated using eqn (4).

$$IE_{PS}\% = 1 - \frac{i_{corr}}{i_{corr}^{\circ}} x\ 100 \quad (3)$$

where icorr is the current density for the inhibited solution and i_{corr}° is the current density of the uninhibited solution.

d) Surface Examination

The morphologies of the corroded metal surfaces after 150 hours of immersion time were inspected by SEM on Vega Tescan scanning electron microscope, resolution 80 Angstroms, magnification range: 10 X – 180 000 X, SE detector, HV 20.0 kV.] while the energy dispersive X-ray emission spectroscopy (EDS) were recorded in a VG TC INCA PentaFET x3 spectrometer with Mg K_X-ray source (1486.7 eV photons energy) operated at 300 W (accelerating voltage 12.5 kV, emission current 24 mA). A detailed procedure for the surface examination is reported in [33]

III. Results and Discussion

a) Gasometric technique

Fig. 1 shows the gas evolution-time curves for the corrosion of AISI 316L in 3.5% NaCl solution without and with different concentrations of SM leaf extracts. As observed from this figure, by increasing the concentration of SM, the volume of hydrogen gas evolved with time decreased. The stepwise progression of the plot indicates that AISI 316L surface experienced stages of passivation as the surface corrosion proceeds and the chloride ions usually situate at the bottommost areas of localized areas actually compromise the stability of the passive films formed on the steel surface [18]. However, with increasing SM leaf extracts concentration clearer and stable passivation periods were seen to be maintained suggesting that SM leaf extracts did enhance the compactness of the formed surface films which hindered the intrusion of further chloride ions thereby reducing corrosion rate. The cathodic reaction for hydrogen evolution of stainless steel corrosion in near neutral medium may require several steps involving either a chemical recombination mechanism and/or electrochemical recombination mechanism [19] where majority of pre-adsorbed atomic hydrogen will recombine to form molecular hydrogen which bubbles off of the surface. From the calculated corrosion rate 27.17, 45.65 and 72.83 % for 0.01, 0.1 and 1.0 g/L respectively, it is clear that the release of molecular hydrogen follows steel dissolution however, inhibition efficiency value for 1.0 g/L SM leaf extract indicates that its constituent molecules did obstruct the cathodic reaction via adsorption on the anodic substrate of AISI 316L. This reduced anodic dissolution and probably, the constituent molecules even got trapped within the metal/solution interface either by complex chelate formation and/or electron transfer [20].The %IE suggests that SM leaf extracts did obstruct the cathodic hydrogen reduction reaction via formation of surface films which indeed induced some modifications in the system double layer and diffusion boundary as a result of the adsorbed extracts' constituent at the metal/corrodent interface [21-24] and in turn enhanced the steel passivation properties.

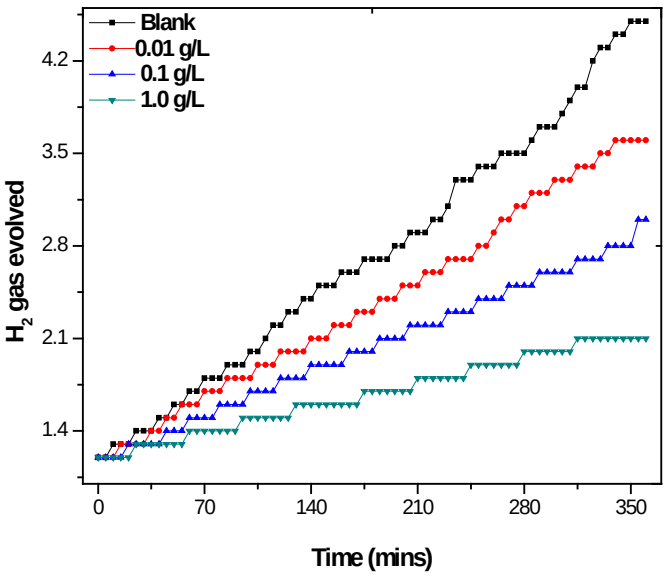

Fig. 1: Variation of H_2 gas evolved with time for AISI 316L in 3.5% NaCl solution without and with SM leaf extracts

b) Potentiodynamic polarization results

Table 1: Corrosion parameters for AISI 316 L in 3.5% NaCl solution in the absence and presence of SM leaf extracts

Solution	Parameters			
	i_{corr}	E_{corr}	θ	%IE
Blank	112.25	-110.02	--	--
0.1 g/L	16.32	109.32	0.8546	85.46
1.0 g/L	15.85	251.96	0.8588	85.88

Fig. 2 depicts the potentiodynamic polarization curves for AISI 316L in uninhibited and inhibited 3.5% NaCl solution while the polarization data obtained by extrapolating the Tafel segments of the anodic and cathodic curves are listed in Table 1.As clearly seen form the curves, the rest potential shifted toward the more positive potential with the inhibited solution which increased with inhibitor concentration indicating a preponderate anodic protection. This behaviour is characteristic of spontaneous blocking of chloride ions attack on the protective passive films associated with the steel hence reducing anodic dissolution of the steel. Spontaneous passivation was observed in the anodic branch of the polarization scan of AISI 316L in 3.5% NaCl solution in the presence of SM leaf extracts with a marginal increase in corrosion current density and decreased passive current density values. However, minimal anodic reaction occurred at higher corrosion potential as the concentration of SM leaf extracts increased recording a decrease in corrosion current density till about 0.98 mV. At this point, pitting action of the chloride ions initiate a breakdown of the passive film formed on AISI 316L surface aiding further dissolution of the metal [25-26].

According to Refaey *et al*[27], the passive layer formed on stainless steel in aqueous NaCl solutions consists of Fe_2O_3, Cr_2O_3 and FeCl while the corrosion resistant properties are determined by an inner Cr_2O_3 layer and outermost Fe_2O_3 layer that feature poor barrier. Examination of the potential-current plot reveals that the presence of chloride ions in the system is clearly seen to interferes with the steel surface property via introducing a discrete surface process due to local surface activation following passivity breakdown though in the presence of the inhibitor, the surface features were enhanced. The observed increase in current density above 0.98 mV could be explained on the grounds that the pre-adsorbed FeCl layer is oxidized to $FeCl^+$ whose action resulted in nucleation of pits on AISI 316L surface [24]. This made the current density to increase with increasing corrosion potentials in the positive direction before oxygen evolution [28] and sharplyrose at about 1.08 mV denoting breakdown of the passive layer and nucleation of pitting corrosion an indication of dissolution of the adsorbed inhibitor complex ligands and dissolution of the oxide films. Although a relatively good consensus prevails on the corrosion products that form on stainless steel surfaces under chloride ion bearing conditions and on the reaction processes particularly as it is known that the presence of chloride ions enables the formation of adsorbates and complexes [29-31]. SM leaf extracts were seen to

reduce corrosion rate of AISI 316L compared to the uninhibited medium through formation of complex chelating ligands on the metal surface thereby played down on the formation of chloride ion adsorbate and complexes thereby enhancing the compactness of the surface film. This infers that the inhibitor did modify the charge transfer mechanisms at the electrolyte/metal interface and electric double layer region with an overall result of enhancing the metals' passivation potential as it gave an optimal protection efficiency of 85.9% at 1.0 g/L. However, considering the combined observations on the changes in Tafel slopes, current densities, and the direction of change in corrosion potentials, the inhibition process appeared to be mixed type in nature with pronounced anodic effects [24,32]. The significant anodic and cathodic branch shift of the potential-current plot to positive potential and decrease in current density with increase in inhibitor concentration suggests formation of a stronger film protective layer on AISI 316L surface.

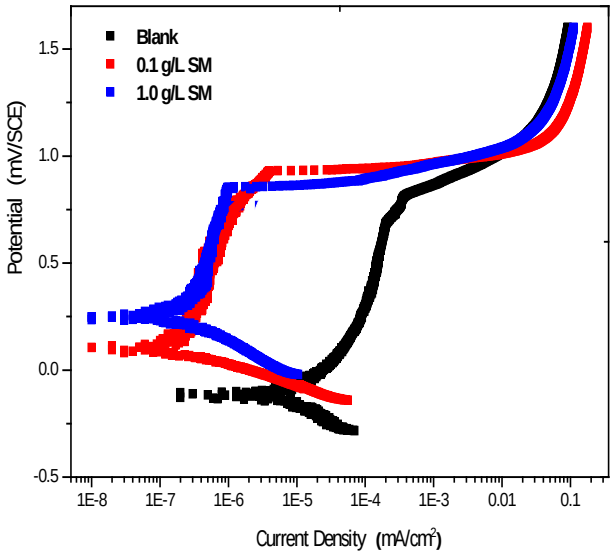

Fig. 2: Potentiodynamic polarization curves for AISI 316L in 3.5% NaCl solution in the absence and presence of SMleaf extracts

c) SEM studies and elemental analysis

Surface examination of the AISI 316L specimen exposed to a 3.5% NaCl solution in the uninhibited and inhibited solutions after 150 h was performed by SEM analysis as shown in the micrographs (Fig. 3). It is clearly shown in Fig. 3athat the action of chloride ion strongly damaged AISI 316L surface in the uninhibited solution due to the metal dissolution and pitting corrosion. The metal surface in uninhibited solution revealed depth of pits at various points and groove cracks along boundary grains. In contrast, the appearance of the steel surface is different in the inhibited solution with 1.0g/L SM leaf extracts after150 h immersion time. As observed from Fig. 3b, the steel surface improved greatly in the inhibited solution with reduced density cracks and no pits were seen in comparison with the surface of uninhibited solution. This observation could be interpreted as the inhibitor forming complex ligands with the metal surface via adsorption and prevented formation of chloride adsorbates and complexes such as FeCl formation and its oxidation. The observed damaged steel surface discloses that the formed chloride adsorbates on the surface further stationed as nucleation centers that further enhanced Fe ions migration from the surface into the bulk medium. SEM analysis further supports the fact that SM leaf extracts strengthened the compactness of the passive film formed thereby enhancing the passivation potentials of AISI 316L.

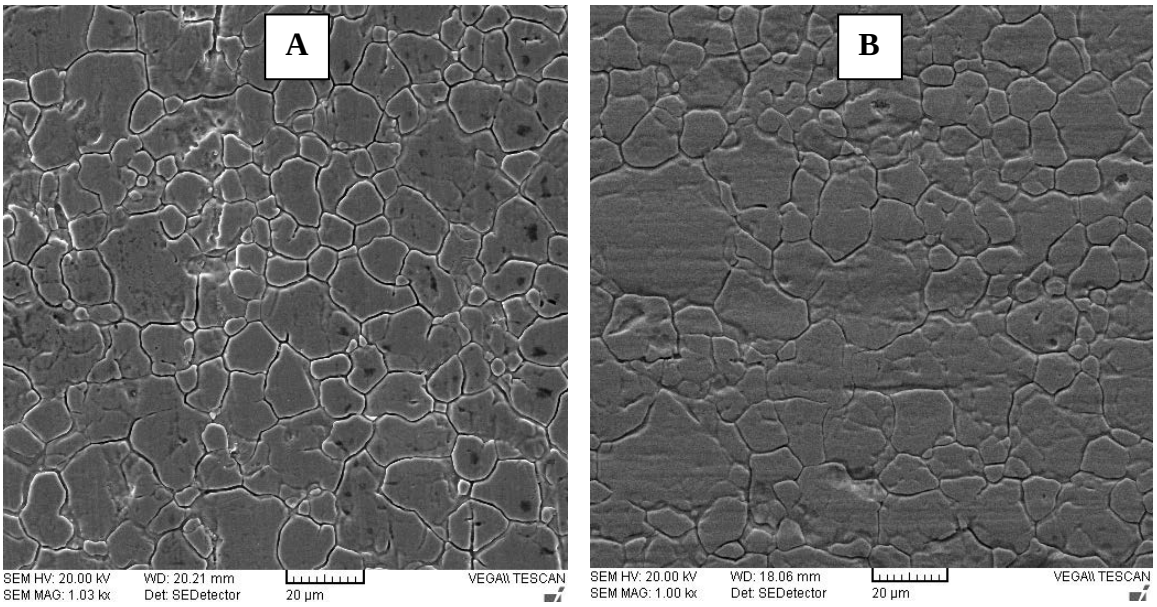

Fig. 3: SEM micrographs of AISI 316L surface after immersion for 150 h in 3.5% NaCl solution (a) uninhibited (b) inhibited

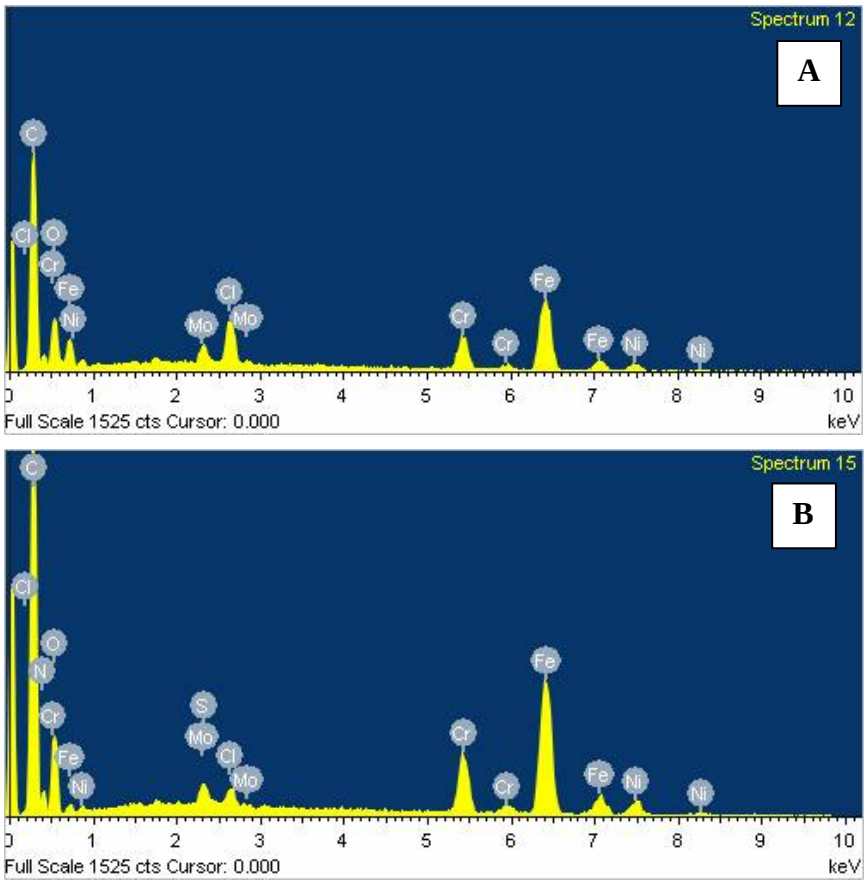

Fig. 4: EDS analysis of the corrosion product on AISI 316L surface in 3.5% NaCl solution (a) uninhibited (b) inhibited

Fig. 4 shows the spectra for AISI 316L in uninhibited and inhibited 3.5% NaCl solution while Table 2 reports the surface elemental composition and atomic% values. The elemental analysis for AISI 316L specimen in inhibited 3.5% NaCl solution discloses the presence of appreciable amount of oxygen and nitrogen atoms as well as traces of sulphur signifying that the leaf extract species did encounter bonding with the steel surface. The data revealed that the amount of Na and Cl atoms at the surface reduced in the presence of the inhibitor supporting the fact that the inhibitor reduced available active sites on the steel surface for corrosion.

Table 2 reports the atomic% values, weight% and application concentration for the uninhibited and inhibited solution. The atomic% values of oxygen in both media indicate that it played a major role at the surface film formation via Fe_2O_3 and Cr_2O_3 [27]. However, in the inhibited system, the reduced atomic representation of oxygen and better resulting surface suggests that there were complex chelating ligands on the surface that enhanced the compactness of the surface films such as $(N\text{-}Fe\text{-}O)_{ads}$, (N-Fe-S)ads and $(Fe\text{-}Cl\text{-}TD)_{ads}$[33]. This is supported with the energy dispersive spectrum in Fig. 4 showing peaks of the elements and elemental composition values in Table 2. The presence of Fe, Cr and O atoms in the analyzed corrosion products on the surface is consistent with the formation of a passivating layer of oxides although, hydroxides are not ruled out in serving passivation roles under various aqueous conditions [34] which of course, are enhanced by the inhibitor. Moreover, the low peaks along with reduced atomic representation for Fe, Cr, Na and chlorine atoms in the inhibited medium could only mean that the inhibitor molecules had a strong presence at the steel surface and replaced chloride ions on the surface thereby reduced the corrosive attacks on the steel surface. Hence, EDS analysis confirms that the protective film composed of strongly adhered inhibitor molecules on the metal surface via forming complex chelating ligands and inhibitor-chloride-complex deposits that mitigated the corrosion reaction which is consistent with results obtained from gasometric, electrochemical and SEM analysis.

Table 2: Elemental analysis value of AISI 316L surface corrosion products formed in 3.5% NaCl solution with and without SM leaf extracts

	Inhibited surface			Uninhibited surface		
Element	App Conc.	Weight%	Atomic%	App Conc.	Weight%	Atomic%
C K	114.07	52.80	69.68	7.00	16.10	29.86
N K	2.37	8.39	9.50	--	--	--
O K	17.07	13.10	12.98	33.03	36.57	50.90
Na K	1.06	0.55	0.38	0.42	0.95	0.92
Si K	0.77	0.34	0.19	--	--	--
S K	2.30	0.93	0.46	--	--	--
Cl K	0.91	0.43	0.19	0.51	0.80	0.50
Cr K	9.82	4.27	1.30	5.83	7.85	3.36
Fe K	34.07	16.24	4.61	20.61	30.81	12.29
Ni K	4.43	2.15	0.58	2.46	3.78	1.44
Mo L	1.61	0.79	0.13	1.86	3.13	0.73
Totals		100.00			100.00	

d) Computational studies

The electrochemical forces among molecular sites stabilize the orbitals in ways in which satisfy the linear combination of atomic orbitals merger [35]. Table 3 records computed quantum chemical analysis include the energy of highest occupied molecular orbital (EHOMO), energy of lowest unoccupied molecular orbital (ELUMO), EHOMO–ELUMO energy gap (ΔE) and binding energy obtained by means of molecular dynamics. The charge density plot of SM leaf extract constituents for EHOMO, ELUMO and total electron density are presented in Fig.5ashowing electron clouds at active sites within individual molecule for interaction with the metal surface. Interactions between frontier orbitals lead to the formation of a transition state with the HOMO as the outermost orbital having high energy which could act as electron donor while the LUMO is the innermost orbital which accepts electron through its vacant room [36]. This implies that low lying ELUMO induces an electrophile behaviour from the metal to the molecule whereas high EHOMO would preferably undergo electron transfer vacant d orbital of the metal surface resulting in a donor-acceptor bond hence, formation of chelating ligand bond via adsorption on the metal surface. The bond formed uses up available sites on the metal surface and reduce further intrusion of reactive species.

Herrag *et al* [37] reported that excellent corrosion inhibitors are usually molecules that not only offer electrons to unoccupied orbital of the metal but also accept free electrons from the metal using their anti-bond orbital to form stable chelates. Accordingly Xia *et al* [38] stated that low lying LUMO induces a backdonation of charge from the metal to the molecule whereas high EHOMO facilitates adsorption by influencing the transport process through the adsorbed layer. This implies that SM leaf extract constituents do possess these qualities are good inhibitors as confirmed by the experimental results. It is well known fact that corrosion inhibitors which not only offer electrons to the unfilled d orbital but also have unoccupied orbitals with the tendency of accepting electrons from d-orbital of metal to form stable chelates are considered excellent inhibitors [39]. Examination of Fig. 5a reveal that the HOMO orbital of 1,2-15,16-diepoxyhexadecane molecule were found with high electric density at the oxy- O16 atom with modest electric density at oxy- O18 atom both with lone electron pairs available to donate to the d-orbital of the metal surface and hence provide adsorption centers with the metal surface while its

LUMO orbital were found at the same sites but spread from C8 to C13 atom indicating available sites through which the molecule could accept electrons from the metal resulting in a donor/acceptor bond. This reveals that the molecule has the propensity to adsorb on the metal via donation/backdonation coordinate bond forming ligands that protect the metal surface at the sites where they are attached. The very high value of ELUMO (Table 3) suggests that the molecule had weak electrostatic interaction with the metal via the carbon atoms. The HOMO orbital of 1,6-anhydro-beta-d-talopyranose had its electric density localized around O7, O10, O9 and O11 atoms indicating sites through which the molecule could adsorb and donate electrons to the metal surface while its LUMO orbital were located at same sites but also included the O1 however, the low value of ELUMO indicated that the molecule had affinity for electrons from the metal surface. The low value of EHOMO reveals low surface coverage as expected seeing that the molecule does not have planar geometry (Fig. 5a) hence, could not adsorb on a flat orientation. Examination of the HOMO and LUMO orbital, 2,4-hexadiyne-1,6-diol reveal that the electron rich triple bonds serves as sites for HOMO and LUMO electric density with modest electric density around hydroxyl O1, O8 atom for the formation of chelating ligands with the metal surface. However, considering the low ELUMO values in Table 3 with high EHOMO value suggest that the presence of highly electron releasing character of the triple bond and π-OH enhanced greater adsorption migration towards the metal surface. The orbital plot obtained for 3,7-dimethyl-1-octyl methylphosphono-fluoridate showed that the HOMO is localized around the molecule exempting C1, and P2 atom with modest electric density at F13 while the LUMO is situated around C1 to C6 including the hydroxyl hydrogen suggesting the molecule to be of more electron acceptor. This indicates that 3,7-dimethyl-1-octyl methylphosphonofluoridate is preferably adsorbed on the metal surface by electron acceptance via backdonation, rather than by donation of π-electrons to the metal as confirmed by the values in Table 3[40]. Methyl 2-butyl-2-cyclopropene-1-carboxylate and cyclohexyl heptyl had the electric density for HOMO and LUMO located within the same region at the electron rich double bond and lone pair electrons available for donation. The unshared electron pair on the oxygen atoms are weakly basic and can be protonated in acidic or near neutral media, suggesting that the molecule will be attached at the cathodic site thereby forming adsorbed surface film due to electrostatic interaction at the metal/electrolyte interface which hinders cathodic reaction and reduce dissolution of the metal. This electrostatic interaction is suggested to be weak in nature considering the values of energy gap (ΔE) recorded in Table 3. Similarly, Fukui indices density plots reveals that the region of f_k^+ corresponds to the LUMO region of the same molecule whereas the f_k^- region assumes the regions where the HOMO charge densities are high [41].

Fig. 5. A): Electronic structures and Fukui indices for SM leaf extract constituents. B). Electronic properties showing the highest occupied molecular orbitals (HOMO), highest unoccupied molecular orbital (LUMO) and total electron density (TED)

A

Molecule	Optimized structure	Fukui (f_k^-)	Fukui (f_k^+)
1,2-15,16-Diepoxyhexadecane	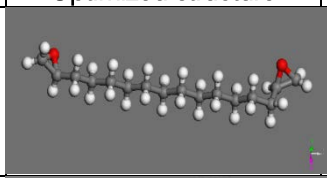	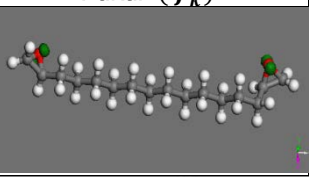	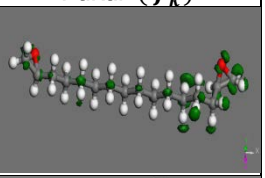
1,6-Anhydro-beta-d-talopyranose	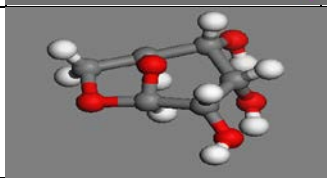	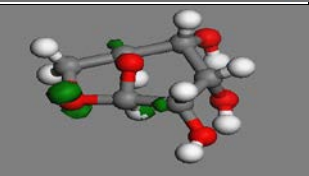	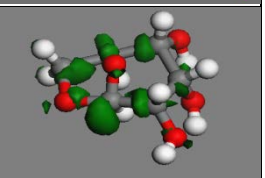
2,4-hexadiyne-1,6-diol	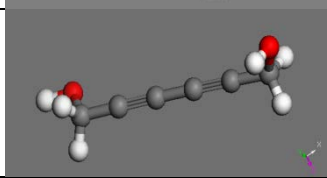	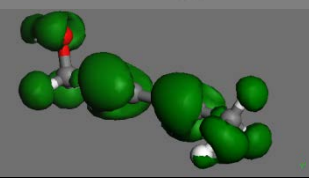	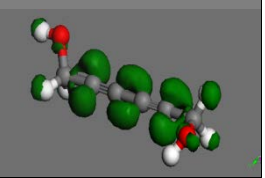
3,7-Dimethyl-1-octyl methyl-phosphonofluoridate	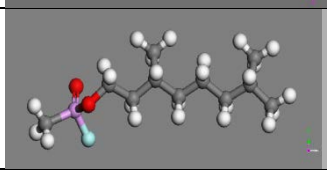	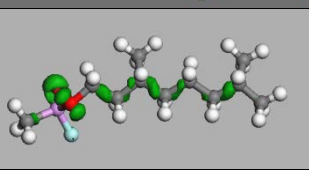	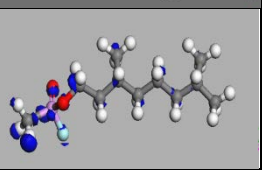

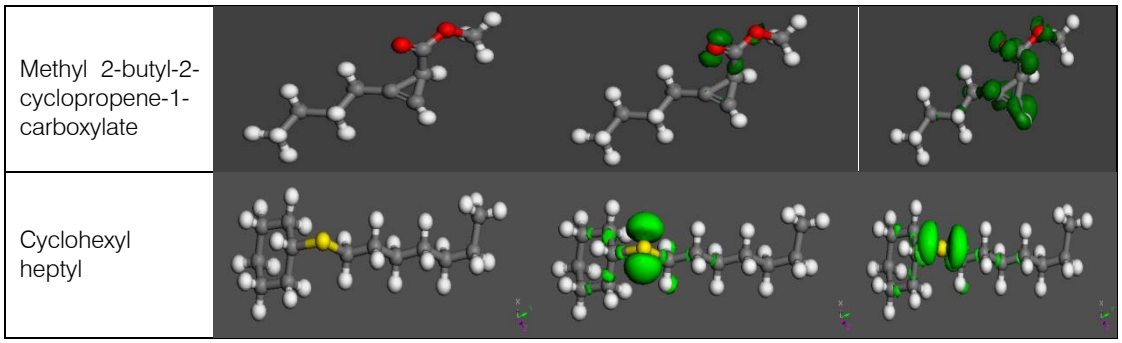

B

Molecule	HOMO	LUMO	TED
1,2-15,16-Diepoxyhexadecane			
1,6-Anhydro-beta-d-talopyranose			
2,4-hexadiyne-1,6-diol			
3,7-Dimethyl-1-octyl methyl phosphonofluoridate			
Methyl 2-butyl-2-cyclopropene-1-carboxylate			
Cyclohexyl heptyl			

The Mulliken population charges reference describes mainly the accumulation of potential energy among different species on which the lattice of electrostatic potential surfaces is ascribed [42] while the Fukui indices which describe reactive sites within a molecule as well as its tendency to accept/donate electrons [43] with the metal surface. Fig. 5b shows the Fukui density plots and molecule optimized structures. The reactive site with tendency to release electrons will be the place where the value of f_k^+ is a maximum, while reactive site for receiptibility of released electrons is controlled by the maximum value of f_k^-. The condensed Fukui functions distinguish each part of the molecule based on distinct chemical behavior of the different substituent functional groups [43]. Fig. 5b shows the Fukui density plots and the reactive sites of 1,2-15,16-diepoxyhexadecane were at O16, O18 and C13atom with Mulliken population charges to be -0.431, -0.428 and -0.204 respectively indicating species with the propensity to form coordinate bond with the metal

surface. 1,6-anhydro-beta-d-talopyranose exhibited the ability to accept electrons at O7, O11, O1 atom from the metal surface Mulliken population charges to be -0.523, -0.445 and -0.417 while the possibility of donating electrons to the vacant sites on the metal via C6, C3 atom with Mulliken population charges +0.307 and +0.104 respectively. The population analysis data shows that O1, O7, O9, O10, O11 atom carries high negative charge indicating their participation in forming coordinate bonds with the metal surface. Analyzing the results obtained for 3,7-Dimethyl-1-octyl methylphosphonofluoridate revealed O12, O3, F13 atoms as sites where the molecule interact via accepting electrons with Mulliken population charges to be -0.573, -0.532, -0.373 respectively while possible electron donation was via through P2 atoms (+1.247) and probable chelating ligand formation as revealed by Mulliken charges. The affinity to donate/accept electrons for 2,4-hexadiyne-1,6-diol was chiefly at O1, O8 atom with Mulliken charges of -0.469 and -0.482 respectively. However, the population analysis had high charges for $f-$ values which suggests that it tends to adsorb on the metal surface via electrostatic electron transfer to form coordinate bonds on a flat orientation and reduce available active sites for corrosion. Methyl 2-butyl-2-cyclopropene-1-carboxylate used C1, C4 and C3 atom for interaction with the metal surface with Mulliken charges of -0.256, +0.470 and -0.156 respectively however, carbon atoms are known to form weak electrostatic bonds with the metal surface. The population charge analysis revealed O5 atom (-0.402) and O6 atom (-0.400) with high negative charges including it as potential zones through which the molecule adsorbed onto metal surface.

The efficiency of an organic compound as a successful inhibitor is mainly dependent on its ability to be adsorbed on the metal surface, which includes of the replacement of water molecule at a corroding interface [15]. To quantitatively evaluate the most suitable adsorption configuration of inhibitor molecule on optimized metal surface cleaved along (110) plane, the adsorption energy (E_{Bind}) was calculated and reported in Table 3. The obtained values show that 1,2-15,16-diepoxyhexadecane and 2,4-hexadiyne-1,6-diol exhibit the most favourable binding energy for SM leaf extract molecular composition during the simulation processes. The high values of binding energy for 1,2-15,16-diepoxyhexadecane and 2,4-hexadiyne-1,6-diol is attributed to existence of planar geometry and favourable electronic properties. Electron rich multiple bonds enhanced electrostatic interaction with the metal surface and the presence of p-π conjugation system at the O atoms resulted in a dissociative adsorption which is favourable to crack intramolecular bond of the adsorbate molecule [44]. Oxy- groups are generally known to hydrolyze in acidic/near neutral solutions which indicate that the molecule is suitable to displace water molecules at the metal surface. The high value of *E*Bind obtained for 2,4-hexadiyne-1,6-diol infers a probable chemisorption as expected which affirms the observed electron donation and backdonation at the same sites. The presence of lone pair electrons on O atoms provided electrons to the unfilled *3d* orbital of the metal surface thereby forming a protective layer via adsorption. Such protective film acts as steric barrier that hinders the reactiveness of corrosive species in the environment coming in contact with the metal surface hence, a mitigation of corrosion process. 1,6-Anhydro-beta-talopyranose exhibited low binding energy despite a number of O atoms present in the molecular structure which confirms that non planar molecular structure engenders low inhibition. Moreover, the energy gap was observed to be low suggesting that the presence of O atoms in the molecule with high population charges offer electrons to the metal surface to form coordinate bonds counteracted the non planar structure to exhibit inhibiting qualities against corrosion. The adsorption orientation of all inhibitor constituent molecules revealed that polarizable atoms in their molecular backbone aligned with vacant sites on the fcc lattice atop the metal surface and virtually avoided contact with the metal atoms along surface. This is expected considering that the electron deficient regions along Fe(110) surface are found within the vacant sites of the crystal plane. This supports the idea that constituent molecules of the present inhibitors did adsorb directly on the metal surface on the basis of donor–acceptor interactions between π-electrons, non-bonding lone pairs of S, O and F atoms and vacant d-orbitals of metal surface [45,46]. The S and N atoms probably formed ligands with the metal through lone pair electrons which acts as thin films that protect the steel surface along with the oxides of the metal.

Table 3: EHOMO, ELUMO, energy gap (Δ*E*), and Binding energy (*E*Bind) from the molecular dynamic simulations for SM leaf extracts molecular compositions

Property	EHOMO (Ha)	ELUMO (Ha)	*ΔE* (Ha)	*E*bind (Kcal/Mol)
1,6-Anhydro-beta-talopyranose	-0.1898	-0.0587	0.1311	-87.98
1,2-15,16-diepoxyhexadecane	-0.2263	0.0364	0.2627	-159
2,4-hexadiyne-1,6-diol	-0.2211	-0.0746	0.1465	-159
3,7-Dimethyl-1-octyl methylphosphonofluoridate	-0.2639	-0.0192	0.2447	-128
Methyl 2-butyl-2-cyclopropene-1-carboxylate	-0.2187	-0.0468	0.1719	-100.6
Cyclohexyl heptyl	-0.1807	0.0035	0.1842	-139.8

IV. Conclusion

The purpose of this study was to evaluate SM extracts for corrosion protection of AISI 316L in 3.5% NaCl solution and to attempt explanation of the mechanism of action. Obtained results in the study have shown that corrosion protection is attained because of the extracts' constituents being adsorbed on AISI 316L surface with pronounced effect on the passivation mechanism. This passivation enhancing effect was ascribed to the adsorbed organic matter which did modify the nature of electron transfer processes across the metal/solution interface. Quantum chemical simulations where used theoretically investigate the interaction of the extract constituents with the metal at the molecular level and data obtained revealed a strong and spontaneous adsorption of the constituents on Fe(110) slab, which should be responsible for the observed corrosion inhibiting efficacy of SM leaf extracts.

Acknowledgements

The authors gratefully acknowledge funding from the Nigerian Tertiary Education Trust Fund (TETFund); under grant no. TETFUND/DESS/UNI/BAU/RP/VOL.XII. TETFund Research allocation for the Abubakar Tafawa Balewa University Bauchi. Prof. E.E. Oguzie is acknowledged for mentoring one of the authors.

References Références Referencias

1. Manivannan M., Rajendran S. and Suriya Prabha A. inhibitors for prevention of corrosion of metals in sea water – an overview *Eur. Chem. Bull. 2012, 1(8), 317-329.*
2. El-Sayed M. Sherif (2012) Corrosion of duplex stainless steel alloy 2209 in acidic and neutral chloride solutions and its passivation by ruthenium as an alloying element. *Int. J. Electrochem. Sci.*, 7: 2374 – 2388.
3. Ai-Mayouf, A.M., Al-Ameery, A.K. and Al-Suhybaiu, A.A. (2001). Comparison of Inhibition efficiency of some azoles on corrosion of type 304 stainless steel in acidic solutions, *British Corrosion Journal*. 36(2): 127-139.
4. Singh A.K., Chaudharyb V. and Sharma A. (2012) Electrochemical studies of stainless steel corrosion in peroxide solutions. *Portugaliae Electrochimica Acta*, 30(2): 99-109 DOI: 10.4152/pea.201202099
5. Oguike R.S. (2014) Corrosion Studies on Stainless Steel (Fe6956) in Hydrochloric Acid Solution. *Advances in Materials Physics and Chemistry*, 4, 153-163.
6. Gasparac R. and Martin C. (2001) Investigations of the Mechanism of Corrosion Inhibition by Polyaniline. Polyaniline-Coated Stainless Steel in Sulfuric Acid Solution. *Journal of the Electrochemical Society*, 148: 4-11.
7. Tomic M.V., Pavlovic M.G. and Jotanovic M. (2002) Protection of copper and its alloys using corrosion inhibitors: Literature Review. *Quality of Life* 1(1):72-89.
8. Blajiev O. and Hubin A. (2004) Inhibition of copper corrosion in chloride solutions by amino-mercapto-thiadiazol and methyl-mercapto-thiadiazol: an impedance spectroscopy and a quantum-chemical investigation, *Electrochim. Acta* 49 2761–2770.
9. Yan C.W., Lin H.C. and Cao C.N. (2000) Investigation of inhibition of 2-mercaptobenzoxazole for copper corrosion, *Electrochim. Acta* 45 2815–2821.
10. Khaled K.F. (2011) Studies of the corrosion inhibition of copper in sodium chloride solutions using chemical and electrochemical measurements, *Mater. Chem. Phys*. 125 427–433.
11. Fonsati M., Zucchi F. and Trabanelli G. (1988) Study of corrosion inhibition of copper in 0.1 M NaCl using the EQCM technique, *Electrochim. Acta* 44 311–322.
12. Dafali A., Hammouti B., Mokhlisse R. and Kertit S. (2003) Substituted uracils as corrosion inhibitors for copper in 3% NaCl solution, *Corros. Sci*. 45 1619–1630.
13. Hepel M. and Cateforis E. (2001) Studies of copper corrosion inhibition usingelectrochemical quartz crystal nanobalance and quartz crystal immittancetechniques, *Electrochim. Acta* 46 3801–3815.
14. Chuan-chuan Li, Xiao-yu Guo, Shu Shen, Ping Song, Ting Xu, Ying Wen, and Hai-Feng Yang

(2014) Adsorption and corrosion inhibition of phytic acid calcium on the copper surface in 3 wt% NaCl solution *Corrosion Science* 83 147–154

15. Oguzie E.E. (2008) Evaluation of the inhibitive effect of some plant extracts on the acid corrosion of mild steel. *Corrosion Science*. 50:2993-98
16. Jokar M., Shahrabi T.F. and Ramezanzadeh B. (2016) Electrochemical and surface characterizations of *Morus alba pendula* leaves extract (MAPLE) as a green corrosion inhibitor for steel in 1 M HCl. *Journal of Taiwan Institute of Chemical Engineers*, 001: 1–17
17. Ghareba S. and Omanovic S. (2010) Interaction of 12-aminododecanoic acid with a carbon steel surface: towards the development of 'green' corrosion inhibitors, *Corros. Sci*. 52 2104–2113
18. Abdallah, M. (2003) Corrosion behaviour of 304 stainless steel in sulphuric acid solutions and its inhibition by some substituted pyrazolones. *Materials Chemistry and Physics*, 82: 786–792
19. Singh A., Singh V.K. and Quraishi M.A. (2010) aqueous extract of kalmegh leaves as green inhibitor for mild steel in hydrochloric acid solution, *International Journal of Corrosion*, Hindawi Publishing, article ID 275983.
20. Elkashlan H.M. and Ahmed A.M. (2012) Anodic corrosion of copper in presence of organic compounds. *Int. J. Electrochem. Sci.*, 7: 5779 – 5797
21. Hasanov R., Bilge S., Bilgic S., Gece G. and Kılıc Z. (2010) Experimental and theoretical calculations on corrosion inhibition of steel in 1 M H_2SO_4 by crown type polyethers. *Corrosion Science*, 52: 984–990
22. Satapathy A.K., Gunasekaran G., Sahoo S.C., Amit K. and Rodrigues P.V. (2009) Corrosion inhibition by Justicia gendarussa plant extract inhydrochloric acid solution. *Corrosion Science*, 51: 2848–2856
23. Edison T.J.I. and Sethuraman M.G. (2013) Electrochemical investigation on adsorption of fluconazole at mild steel/hcl acid interface as corrosion inhibitor. *ISRN Electrochemistry* Vol. 2013, Article ID 256086 http://dx.doi.org/10.1155/2013/25608
24. Gileadi E. and Kirowa-Eisner E. (2005) Some observations concerning the Tafel equation and its relevance to charge transfer in corrosion, *Corros. Sci*. 47 3068– 3085
25. Singh V.B. and Ray M. (2007) Effect of H_2SO_4 addition on the corrosion behaviour of AISI 304 austenitic stainless steel in methanol-HCl solution. *Int. J. Electrochem. Sci.*, 2: 329 – 340
26. Finsgar M., Fassbender S., Nicolini F. and Milošev I. (2009) Polyethyleneimine as a corrosion inhibitor for ASTM 420 stainless steel in near-neutral saline media, *Corros. Sci*. 51 525–533
27. Refaey S.A.M., Taha F. and Abd El-Malak A.M. (2006) Corrosion and inhibition of 316L stainless steel in neutral medium by 2-Mercaptobenzimidazole. *Int. J. Electrochem. Sci*., 180-91
28. Nesic Srdjan (2007) Key issues related to modelling of internal corrosion of oil and gas Pipelines - A review. *Corrosion Science*, 49: 4308–4338
29. Ameer M.A. and Fekry A.M. (2010) Inhibition effect of newly synthesized heterocyclic organic molecules on corrosion of steel in alkaline medium containing chloride. *International Journal of Hydrogen Energy*, 35: 11387
30. Mabrour J., Akssira M., Azzi M., Zertoubi M., Saib N., Messaoudi A., Albizane A. and Tahiri S. (2004) Effect of vegetal tannin on anodic copper dissolution in chloride solutions, *Corros. Sci*. 46 1833–1847.
31. Hu L.C., Zhang S.T., Li W.H. and Hou B.R. (2010) Electrochemical and thermodynamic investigation of diniconazole and triadimefon as corrosion inhibitors for copper in synthetic seawater, *Corros. Sci*. 52 2891–2896.
32. DeBerry, D.W. (1985) Modification of the electrochemical and corrosion behavior of stainless steels with an electroactive coating. *Journal of the Electrochemical Society*, 132: 1022-1029
33. Oguike R. S., Shibdawa A. M., Tafida U. I., Boryo D. E. A. Omizegba and F. I. (2017) Application of ethanol extracts of *Tapinanthus dodoneifolius* to inhibit annealed carbon corrosion in 2 M HCl and 3.5% nacl solutions. *European Journal of Chemistry* 8 (2): 168 – 173, dx.doi.org/10.5155/eurjchem. 8.2.168-173.1558
34. Chen Y.Y., Chou L.B. and Shih H.C. (2006) Factors Affecting the electrochemical behavior of stress corrosion cracking of alloy 690 in chloride environments. *Materials Chemistry and Physics*, 97, 37-49
35. Awad M.K., Mustafa M.R. and Abo Elnga M.M. (2010) Computational simulation of the molecular structure of some triazole as inhibitors for the corrosion of metal surface. *J. Mol. Struct*. (THEOCHEM) 959(13): 66-74
36. Kosari A., Moayed M.H., Davoodi A., Parvizi R., Momeni M., Eshghi H. and Moradi H. (2014) Electrochemical and quantum chemical assessment of two organic compounds from pyridine derivatives as corrosion inhibitors for mild steel in HCl solution under stagnant condition and hydrodynamic flow. *Corrosion Science*, 78: 138–150
37. Herrag L., Hammouti B., Elkadiri S., Aouniti A., Jama C., Vezin H., and Bentiss F. (2010) Adsorption properties and inhibition of mild steel corrosion in hydrochloric solution by some newly synthesized diamine derivatives: experimental and theoretical investigations. *Corrosion Science*, 52: 3042–3051
38. Xia S., Qiu M., Yu L., Liu F. and Zhao H. (2008) Molecular dynamics and density functional theory

study on relationship between structure of imidazoline derivatives and inhibition performance. *Corrosion Science*, 50(7): 2021–2029

39. Abiola O.K., Oforka N.C., Ebenso E.E. and Nwinuka N.M. (2007) Eco-friendly corrosion inhibitors: The inhibitive action of *Delonix regia* extract for the corrosion of aluminum in acidic media, *Anti-Corrosion Methods and Materials*, 54(4): 219–224
40. Wang D.X. and Xiao H.M. (2000) Quantum chemical calculation on chemical adsorption energy of imidazolines and iron atom. *Journal of Molecular Science*, 16: 102–105
41. Njoku D. I., Ukaga I., Ikenna O.B., Oguzie E. E., Oguzie K. L. and Ibisi N. (2016) Natural products for materials protection: Corrosion protection of aluminum in hydrochloric acid by Kola nitida extract *J. Molecular Liquids* 219 417–424
42. Susithra G., Ramalingam S., Periandy S. and Aarthi R. (2018) Molecular structure investigation towards pharmacodynamic activity and QSAR analysis on hypoxanthine using experimental and computational tools *Egyptian Journal of Basic and Applied Sciences* 5 313–326
43. Khaled K.F., Abdel-Shafi N.S. and Al-Mobarak N.A. (2012) Understanding corrosion inhibition of iron by 2-thiophenecarboxylic acid methyl ester: Electrochemical and computational study. *Int. J. Electrochem. Sci*., (7): 1027 – 1044
44. Rodrıguez-Valdez L. M., Martinez-Villafane A. and Glossman-Mitnik D. (2005) Computational simulation of the molecular structure and properties of heterocyclic organic compounds with possible corrosion inhibition properties. *Journal of Molecular Structure*: THEOCHEM 713 (1–3): 65–70
45. Khaled K.F. (2011) Modeling corrosion inhibition of iron in acid medium by genetic function approximation method: A QSAR model. *Corrosion Science*, 53: 3457–3465
46. Kar P.K. and Singh G. (2011) Evaluation of nitrilotrimethylene phosphonic acid and nitrilotriacetic acid as corrosion inhibitors of mild steel in seawater. *ISRN Materials Science* Volume 2011, Article ID 167487 doi:10.5402/2011/167487